nitrogen

MDPI

Article

Nitrogen Transformation Kinetics of β-Glucan and Nucleotide Supplementation in a Zero-Water-Exchange Aquaculture System

Seto Sugianto Prabowo Rahardjo [1,*], Rani Yuwanita [1], I Made Dedi Mahariawan [1], Heny Suprastiyani [1], Arum Pratiwi [2], Asep Ridwanudin [3] and Anik Martinah Hariati [1]

[1] Aquaculture Study Program, Faculty of Fisheries and Marine Science, Brawijaya University, Jl. Veteran, Malang 65145, East Java, Indonesia; raniyuwanita@ub.ac.id (R.Y.); imd_mahariawan@ub.ac.id (I.M.D.M.); henysuprastyani@ub.ac.id (H.S.); a_hariati@ub.ac.id (A.M.H.)

[2] Sustainable Agricultural Extension Department, Agricultural Development Polytechnic of Malang, Jl. Dr. Cipto Bedali, Lawang 65216, East Java, Indonesia; arumpratiwi@polbangtanmalang.ac.id

[3] Research Center for Applied Zoology, National Research and Innovation Agency, Cibinong 16911, West Java, Indonesia; asep046@brin.go.id

* Correspondence: seto.wre@ub.ac.id

Abstract

Nitrogen is a major challenge in zero-water-exchange (ZWE) aquaculture systems. This study examined the effects of dietary β-glucan and nucleotides on nitrogen transformation dynamics, oxidative stress responses, and environmental stability in Nile tilapia (*Oreochromis niloticus*). A 42-day feeding trial was conducted using diets supplemented with β-glucan ($\beta g_1 = 1\%$, $\beta g_2 = 2\%$, $\beta g_3 = 3\%$) and nucleotides ($Nt_1 = 1\%$, $Nt_2 = 2\%$, $Nt_3 = 3\%$). Final fish weight increased from 21.57 g in the control (Ct) to 28.32 g in Nt_3. Total nitrogen (TN) derived from cumulative feed input reached 264.08 mg/L in Ct, whereas nucleotide treatments showed lower accumulation. NH_4^+ peaked between days 10 and 17, reaching 12.38 mg/L in Nt_3, while NO_2^- peaked at 0.240 mg/L in Nt_1 and declined to 0.03–0.07 mg/L by day 42. NO_3^- accumulated continuously to 31.74–51.47 mg/L, with higher concentrations generally observed in nucleotide treatments. Kinetic modeling yielded higher model-derived apparent nitrogen transfer coefficient (k_a) in β-glucan treatments (1.287–1.690/day) and higher model-derived apparent nitrite-to-nitrate conversion coefficients (k_2) in nucleotide treatments (4.994–5.748/day). Nucleotide supplementation favored apparent nitrite-to-nitrate conversion, whereas β-glucan was associated with greater apparent transfer of ammonia-derived nitrogen toward the modeled residual nitrogen pool.

Keywords: β-glucan; nucleotide; nitrogen transformation; nitrification; oxidative stress; zero-water-exchange aquaculture

Check for updates

Academic Editor: Hanxi Wang

Received: 23 September 2026
Revised: 21 October 2026
Accepted: 26 October 2026
Published: 2 November 2026

Copyright: © 2026 by the authors. Licensee MDPI, Basel, Switzerland. This article is an open access article distributed under the terms and conditions of the Creative Commons Attribution (CC BY) license.

1. Introduction

Aquaculture intensification relies on zero-water-exchange (ZWE) and low-water-renewal systems to improve water-use efficiency and reduce environmental discharge [1]. Under intensive culture conditions, continuous feeding and fish metabolism promote the accumulation of nitrogenous compounds, increasing the risk of water-quality deterioration [2], toxicity [3], oxidative stress [4], and environmental instability [5]. In aquaculture systems, environmental stability depends on the balance between nitrogen loading, microbial transformation, and biological assimilation, making nitrogen regulation a critical component of sustainable aquaculture management [6]. In ZWE systems, dietary protein metabolism primarily drives nitrogen transformation, with nitrogen excreted as total

ammonia nitrogen (TAN) [7]. Under limited water renewal, accumulated nitrogen undergoes continuous transformation through interconnected pathways involving ammonia generation [8], nitrification [9], and biological assimilation [10].

These pathways can be represented by kinetic coefficients derived from temporal nitrogen concentration dynamics, encompassing ammonia input or generation (k_e), apparent NH_3/NH_4^+ to NO_2^- conversion (k_1), apparent NO_2^- to NO_3^- conversion (k_2), and apparent nitrogen transfer to the residual nitrogen pool (k_a) [11]. In this framework, k_e, k_1, k_2, and k_a are defined as model-derived apparent kinetic coefficients that characterize system-level nitrogen transformation dynamics under the experimental conditions. Their integration provides a quantitative framework for describing nitrogen partitioning among ammonia, nitrite, nitrate, and residual nitrogen pools, and for evaluating treatment-related shifts in nitrogen transformation pathways [12]. Consequently, ZWE can be interpreted as biologically driven nitrogen-processing systems in which environmental performance depends on the balance between nitrogen loading and transformation capacity [13].

Functional feed additives (FFAs) are widely used to improve productivity, physiological resilience, and culture performance in intensive aquaculture systems [14]. Among these additives, β-glucans and nucleotides are commonly used as functional immunostimulants that enhance growth performance, feed utilization, and stress adaptation, improving feed efficiency, stimulating physiological adaptation, and enhancing antioxidant and innate defense responses in Nile tilapia (*Oreochromis niloticus*) [15]. FFAs also regulate environmental process dynamics by modifying metabolic turnover [16], nitrogen excretion [17], microbial interactions, and biological assimilation pathways [18]. β-glucan supplementation has been associated with enhanced microbial regulation and nitrogen retention pathways, potentially improving environmental stability and oxidative adaptation [19]. In contrast, nucleotide supplementation stimulates metabolic activity, cellular proliferation, and tissue turnover, thereby increasing nitrogen excretion and accelerating nitrogen cycling processes [20]. However, the influence of FFAs on nitrogen transformation dynamics under ZWE conditions remains insufficiently understood [21].

Nitrogen transformation pathways are closely associated with oxidative stress and environmental stress responses [22]. TAN (NH_3/NH_4^+) and NO_2^- represent major toxic intermediates whose toxicity is strongly influenced by pH and temperature, while NO_2^- can impair oxygen (O_2) transport through methemoglobinemia [23]. Direct toxic effects, these nitrogen intermediates generate reactive O_2 species (ROS) [24], thereby inducing oxidative stress and physiological disturbances in fish [25]. Therefore, evaluating aquaculture systems solely based on nitrogen concentration thresholds may provide limited insight into actual environmental stress conditions [26]. Integrating nitrogen transformation dynamics with oxidative response indicators offers a more mechanistic understanding of how instability in environmental processes influences biological adaptation [27].

Biomarkers such as superoxide dismutase (SOD) [28] and respiratory burst activity, measured by nitroblue tetrazolium (NBT) [29], are important indicators of antioxidant defense and oxidative response under elevated nitrogen exposure. The oxidative stress index (OSI) and ΔSOD/ΔNBT ratio help characterize the balance between oxidative pressure and antioxidant compensation during nitrogen transformation processes [30]. Thus, oxidative response indicators can complement nitrogen-driven environmental stress in aquaculture systems.

Despite the widespread use of β-glucan and nucleotide supplementation, their effects on temporal nitrogen transformation under dynamic feeding conditions remain insufficiently characterized in zero-water-exchange (ZWE) aquaculture systems. Unlike controlled batch-based assessments of physicochemical nitrogen transformation, fish culture involves recurring feed inputs, fish metabolism, and interacting nitrogen pathways that evolve

throughout the rearing period. Understanding these interactions is important for optimizing functional feed strategies while maintaining environmental process stability and reducing nitrogen-associated stress in intensive aquaculture systems. Accordingly, this study integrated β-glucan and nucleotide supplementation with temporal monitoring of nitrogen species, growth performance, feed utilization, and physiological responses in Nile tilapia cultured under ZWE conditions. Temporal changes in TAN, NO_2^-, NO_3^-, and dN were quantified to evaluate nitrogen partitioning and transformation pathways. Model-derived apparent kinetic coefficients were used to characterize treatment-associated differences in nitrogen transformation and partitioning, while oxidative response indicators, including SOD, NBT, and OSI, were evaluated to assess biological responses under the changing nitrogen conditions.

2. Materials and Methods

2.1. Experimental ZWE System and Fish Rearing

This study used juvenile Nile tilapia with an average initial length (Li) of 9.1 ± 0.5 cm and body weight (Wi) of 11.49 ± 0.17 g. The fish were obtained from the Freshwater Fisheries Laboratory, Universitas Brawijaya, Indonesia. Prior to the experiment, fish were acclimated for 7 days under laboratory conditions. The experiment was conducted using an aquarium (50 × 30 × 30 cm), each filled with 30 L of freshwater. A stocking density of 15 fish per aquarium (SD = 1 fish/2 L) was used. The culture system was maintained under ZWE, without external biofloc inoculation or suspended-solid manipulation, throughout the 42-day experimental period. Continuous aeration (flow rate = 0.8 L/min) was provided to maintain O_2 levels. Water temperature was measured daily with a digital thermometer.

2.2. Ethical Statement

This study was conducted in accordance with institutional guidelines for the care and use of experimental animals and was approved by the Health Research Ethics Committee, Faculty of Medicine, Universitas Brawijaya (Approval No. 80/EC/KEPK/05/2025).

2.3. Experimental Diets and Functional Feed Supplementation

The experimental design was completely randomized, with seven treatments and three replicates per treatment. β-glucan (≥95% β-glucan basis, Sigma-Aldrich, St. Louis, MO, USA) and free nucleotides (Nucleosaf; Phileo by Lesaffre, Marcq-en-Barœul, France), derived from Saccharomyces cerevisiae, were used as FFAs in the experimental diet. Seven dietary treatments were applied in this study, consisting of a control diet without supplementation (Ct), β-glucan supplementation at 1% (βg_1), 2% (βg_2), and 3% (βg_3), and nucleotide supplementation at 1% (Nt_1), 2% (Nt_2), and 3% (Nt_3). The FFAs were incorporated into the basal diet at the respective inclusion levels, expressed as a percentage of feed weight. The basal diet was formulated with fish meal (32.8%), soybean meal (10.9%), corn flour (23.4%), rice polish (11.7%), wheat flour (11.7%), soybean oil (2.5%), binder (2.5%), vitamin–mineral premix (2.0%), dicalcium phosphate (2.0%), and sodium chloride (0.5%), then blended with water to a uniform dough, pelleted to a diameter of 3 mm, and dried in an oven at 45 °C until a stable moisture level was reached. Proximate composition was analyzed using standard Association of Official Analytical Chemists procedures [31], approximately 32% crude protein, 4% crude fiber, 6% crude lipid, and 12% ash, with an estimated energy content of 17%. Fish were fed twice daily at 08:00 and 15:00 using a feeding rate of 4% of the average fish biomass per day. Fish weight was monitored weekly by sampling from each aquarium to measure body weight (W_t) and fish length (L_t).

2.4. Nitrogen Transformation Monitoring

Water samples were collected every three days to determine TAN, NO_2^-, and NO_3^-. Water samples were collected every three days to monitor nitrogen dynamics while minimizing water withdrawal and replenishment, thereby reducing potential bias in nitrogen concentrations. TAN concentration was analyzed using the indophenol blue (phenate) colorimetric method (Phenate Method 4500-NH_3-B; APHA, 2017) [31]. Nitrite and nitrate concentrations were determined following the methods described by the American Public Health Association (2017) [32]. Nitrite was measured using the diazotization colorimetric method (Method 4500-NO_2^--B), in which nitrite reacts with sulfanilamide and N-(1-naphthyl)-ethylenediamine dihydrochloride (NED) to form a pink azo dye, which was measured at 543 nm. Nitrate was determined using the cadmium reduction method (Method 4500-NO_3^--E), in which NO_3^- is reduced to NO_2^-, which is then analyzed using the same colorimetric reaction. All reagents were analytical grade and obtained from Sigma-Aldrich.

2.5. Growth Performance and Survival

Fish body weight and total length were measured weekly using a digital balance and measuring board. Growth performance parameters were calculated to evaluate fish growth and feed utilization during the experimental period. Weight gain (WG) was calculated as the difference between the final and initial body weights (Equation (1)). Growth rate (GR) was calculated using the natural logarithm of body weight over time (Equation (2)). Feed conversion ratio (FCR) was calculated as the ratio between total feed intake and biomass gain (Equation (3)), while survival rate (SR) was calculated as the percentage of fish remaining at the end of the experiment relative to the initial stocking number (Equation (4)).

$$WG = W_t - W_i \quad (1)$$

$$GR(g\ day^{-1}) = \frac{W_t - W_i}{t} \quad (2)$$

$$FCR = \frac{FI}{WG} \quad (3)$$

$$SR(\%) = \frac{N_t}{N_i} \times 100 \quad (4)$$

W_t and W_i represent the final and initial fish weight (g), t is the culture duration (days), and N_t and N_i represent the number of fish at the end and beginning of the experiment, respectively.

Nitrogen dynamics in the culture system were evaluated using the nitrogen accumulation rate (NLR), which represents the temporal increase of nitrogen compounds in the water (Equation (5)) [33]. The distribution of total nitrogen (T[N]) in the system was estimated using a nitrogen mass-balance approach (Equation (6)) to analyze nitrogen selectivity (Equation (7)). Nitrogen transformation efficiency (NTE) was calculated to evaluate the efficiency of nitrification in converting ammonia into oxidized nitrogen forms (Equation (8)).

$$NLR = \frac{C_{t2} - C_{t1}}{\Delta t} \quad (5)$$

$$[dN] = T[N] - \left[NH_4^+\right] - [NO_2^-] - [NO_3^-] \quad (6)$$

$$\eta_{Ni}(\%) = \frac{[Ni]_t}{T[N]_t - T[N]_0} \times 100 \quad (7)$$

$$NTE(\%) = \frac{[NO_2^-] + [NO_3^-]}{\left[NH_4^+\right] + [NO_2^-] + [NO_3^-]} \times 100 \quad (8)$$

$$TN = \frac{Fc.Fp.Cp.Nr.1000}{V} \quad (9)$$

C_{t2} is the concentration at time t_2, C_{t1} is the concentration at time t_1, and Δt is the time interval (days). T[N] represents the cumulative feed-derived nitrogen loading estimated from feed consumption and dietary nitrogen content. Fc is the biomass of feed consumed (g), Fp is the crude protein content of the feed (%), Cp is the converted protein (estimated at 16%), Nr is the fish nitrogen retained (~70% for Nile Tilapia), and V is the volume of water. NH_3, NO_2^-, and NO_3^- represent measured nitrogen, ammonia, nitrite, and nitrate concentrations, respectively, while dN represents the residual nitrogen fraction corresponding to other nitrogen forms, such as dissolved organic nitrogen, particulate organic nitrogen, microbial biomass nitrogen, and other unmeasured retained nitrogen fractions. Higher NTE values indicate a more efficient conversion of reduced nitrogen into oxidized nitrogen forms. In this study, NTE values were interpreted as low efficiency (<40%), moderate efficiency (40–70%), and high efficiency (>70%).

The potential toxicity of nitrogen compounds was assessed using the Toxicity Risk Index (TRI; Equation (10)) [34]. A composite toxicity indicator, Composite TRI (CTRI) [35], was calculated as Equation (11). Cumulative toxicity exposure during the experimental period was evaluated using the Area Under the Toxicity Curve (TRI_N, Equation (12)).

$$TRI = \frac{C_{observed}}{C_{threshold}} \quad (10)$$

$$CTRI = TRI_{TAN} + TRI_{NO_2} + TRI_{NO_3} \quad (11)$$

$$TRI_N = \sum TRI_t \times \Delta t \quad (12)$$

The applied threshold values were 1 mg/L for NH_3 [36], 5 mg/L [37] for NH_4^+ [38], 0.5 mg/L for NO_2^- [39], and 50 mg/L for NO_3^- [40]. Each value was assigned to its corresponding nitrogen species. TRI values were interpreted as low risk ($TRI < 1$), moderate risk ($1 \leq TRI < 2$), and high toxicity risk ($TRI \geq 2$).

2.6. Oxidative Stress and Antioxidant Response Analysis

SOD activity in fish blood was analyzed to evaluate the fish antioxidant response. Blood samples were collected from the caudal vein of fish at 0 days (d_0) and 35 days (d_{35}) using sterile syringes. This sampling schedule also minimized interference with routine fish survival monitoring during the experiment. The collected blood was centrifuged at 3000 rpm for 10 min at 4 °C to obtain serum. SOD activity was determined using a colorimetric assay based on the inhibition of NBT reduction by superoxide radicals generated in the xanthine–xanthine oxidase system. The absorbance of the reaction mixture was measured at 560 nm using a spectrophotometer, and SOD activity was expressed as units per milliliter (U/mL) of serum [41].

To assess oxidative balance, we calculated several indices. The Oxidative Stress Index (OSI) was defined as the ratio of ROS to antioxidant capacity (Equation (13)), with higher values indicating greater oxidative stress [42]. The Antioxidant Adaptation Ratio (AAR, Equation (14)) was used to assess the relative antioxidant response [43]. An integrated Biological Stress Response Index (TRI_{bio}) was calculated as Equation (15).

$$OSI = \frac{NBT}{SOD} \quad (13)$$

$$AAR = \frac{SOD}{NBT} \quad (14)$$

$$TRI_{bio} = \left(\frac{NBT_{35}}{NBT_0}\right) + \left(\frac{SOD_{35}}{SOD_0}\right) \quad (15)$$

where subscripts 0 and 35 denote measurements at day 0 and day 35, respectively. Higher TRI_{bio} values indicate stronger physiological responses to oxidative conditions.

2.7. Statistical Analysis

Data were expressed as mean ± standard deviation. The aquarium/tank served as the experimental unit, with three replicate tanks per treatment ($n = 3$). Treatment effects were analyzed using one-way ANOVA with Tukey's HSD test. Time-dependent nitrogen and water-quality parameters were analyzed using repeated-measures ANOVA to assess the effects of treatment, time, and their interaction. Measurements from the same tank were not treated as independent replicates. Statistical significance was set at $p < 0.05$.

3. Results

3.1. Water Quality Monitoring

Figure 1 shows water-quality dynamics during the 42-day culture period; full data are provided in Supplementary File S1. Water temperature remained relatively stable across all treatments, ranging from 24.7–27.8 °C, within the optimal range for Nile tilapia culture and unlikely to affect nitrogen transformation processes. In contrast, pH gradually declined from near-neutral values of 7.2–7.8 to 5.1–6.0 by day 42 (Figure 1a), while DO decreased from approximately 7.0–7.8 mg/L to 4.5–5.8 mg/L (Figure 1b). These trends may reflect continuous feed input and associated decomposition of organic matter and nitrogen transformation under ZWE conditions, which contribute to oxygen consumption and proton production [44].

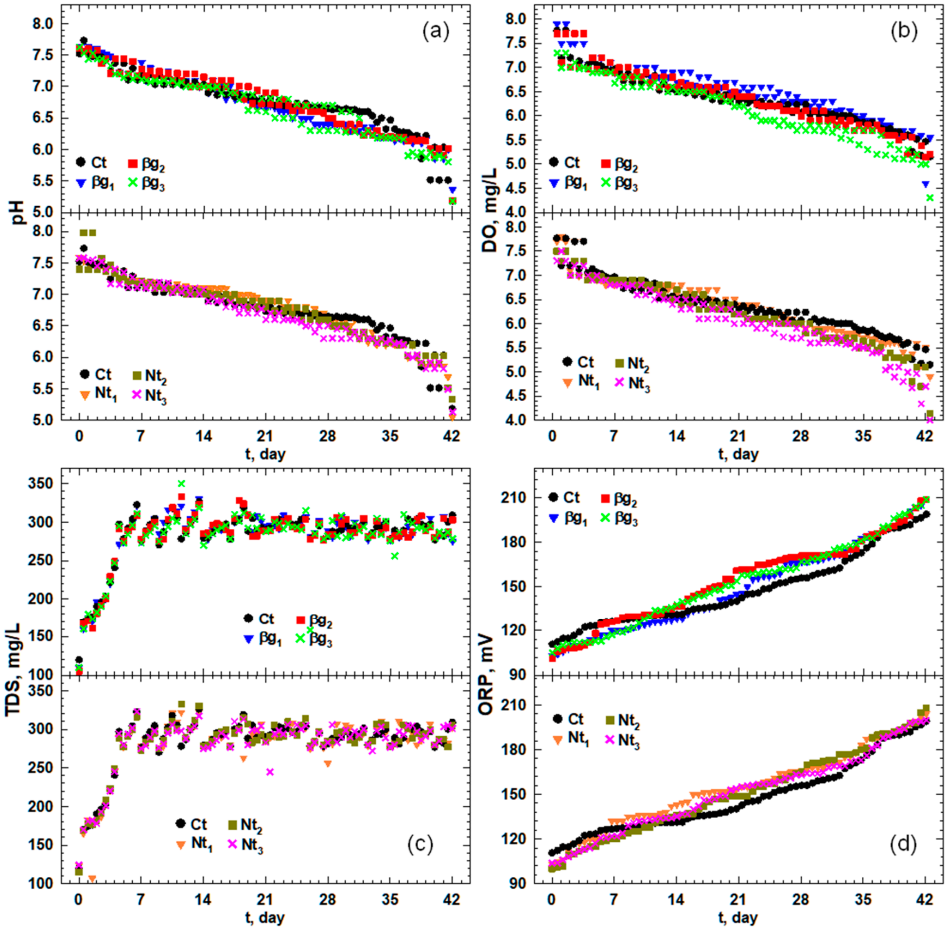


Figure 1. Temporal dynamics of water quality parameters during the 42-day experimental period, including (**a**) pH, (**b**) DO, (**c**) TDS, and (**d**) ORP under β-glucan and Nucleotide, respectively.

TDS increased rapidly during the first week, rising from approximately 110–170 mg/L to 280–320 mg/L before stabilizing for the remainder of the culture period (Figure 1c).

The initial increase reflects the accumulation of dissolved metabolites and feed-derived compounds, whereas the subsequent stabilization indicates the establishment of a dynamic balance among nutrient loading, microbial transformation, and biological utilization. TDS differences among treatments were relatively small, indicating that feed additives had limited effects on dissolved solids accumulation [45].

Oxidation–reduction potential (ORP) increased consistently in all treatments, from approximately 95–110 mV at the beginning of the experiment to nearly 190–210 mV by day 42 (Figure 1d). The positive ORP values, together with sustained DO concentrations, remained predominantly oxidative and favorable for aerobic nitrogen transformation. Although treatment-related differences in pH, DO, TDS, and ORP were generally minor (Figure 1), slightly lower pH and DO in some feed additive treatments reduced nitrogen turnover intensity. Temporal changes in nitrogen loading and microbial activity, rather than large physicochemical differences among treatments, governed water quality dynamics [46].

3.2. Fish Production

Fish growth performance increased consistently across all treatments during the experimental period (Figure 2a,b,e,f). Initial body weight ($W_i = 11.49 \pm 0.17$ g) and length ($W_i = 9.1 \pm 0.5$ cm) were relatively uniform, confirming comparable starting conditions. By day 42, fish weight reached 21.57–28.32 g, with the highest biomass in nucleotide treatments, particularly Nt_3, followed by Nt_2 and Nt_1, whereas Ct had the lowest final weight. GR ranged from 0.469 to 0.644 g/day, with Nt_3 showing the highest rate. A similar pattern was observed for Lt, with final values ranging from 9.72 to 10.45 cm and relatively high growth in Nt_3, up to 0.556 mm/day, although Ct showed the highest length rate at 0.630 mm/day. Nucleotide feed additive consistently resulted in higher Wt, whereas β-glucan treatments exhibited moderate yet stable growth responses, revealing that the dietary additives differentially affect somatic growth performance [47].

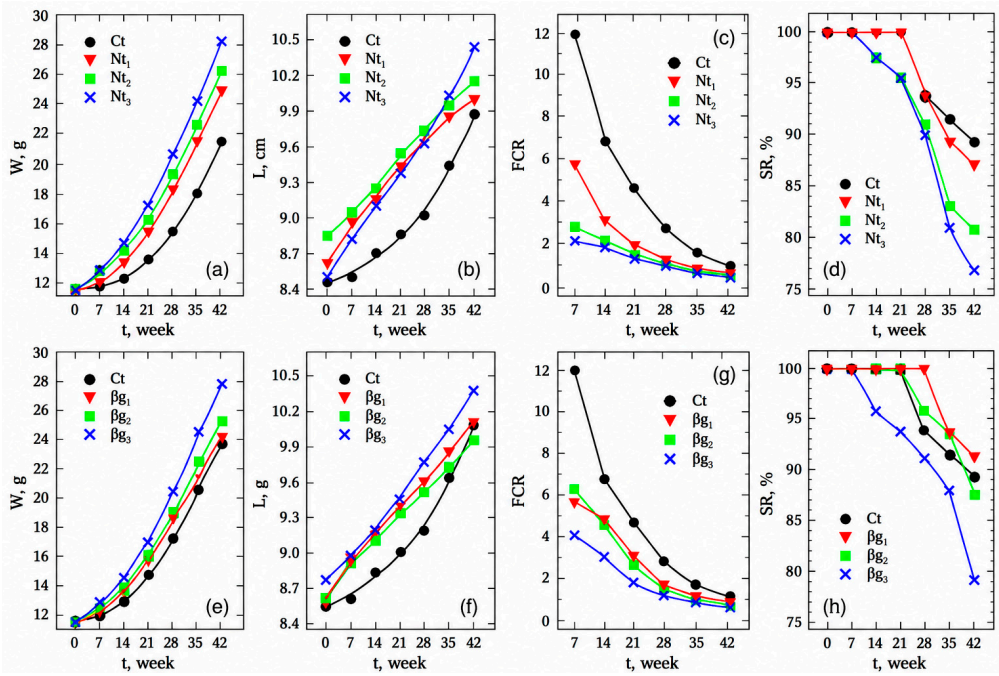


Figure 2. Effect of nucleotide and β-glucan on (**a**,**e**) Growth, (**b**,**f**) Length, (**c**,**g**) feed conversion ratio, and (**d**,**h**) survival rate during the 42-day feeding trial under zero water change.

FCR improved over time in all treatments, as indicated by the progressive decline in FCR (Figure 2c,g). Initial variability (FCR = 2.71–12.00 at day 7) stabilized at lower

values by day 42 (0.99–1.56), with the best efficiency in Nt_3 (0.99), followed by Nt_2 and Nt_1, while Ct remained the least efficient. SR remained at 100% during the early culture phase and gradually declined after day 14, reaching 75.56–91.11% by day 42 (Figure 2d,f). The highest SR was observed in the βg_1 treatment at 91.11%, followed by the Ct and moderate-supplementation treatments, whereas the higher-dose β-glucan and nucleotide treatments (e.g., Nt_3 and βg_3) showed lower SR. Nucleotide supplementation enhanced GR and FCR; moderate β-glucan supplementation improved SR, revealing a trade-off between growth optimization and fish resilience under intensive culture conditions [48].

3.3. Nitrogen

Total nitrogen (T[N]) derived from cumulative feed input increased steadily in all treatments throughout the culture period (Supplementary File S2) due to continuous nitrogen loading into the system. T[N] reached the highest values in Ct, particularly up to 264.08 mg-N/L, followed by βg_1 and βg_2, while nucleotide treatments showed relatively lower accumulation. At an average pH of 6.5, the equilibrium between NH_4^+ and NH_3 favors the ionized form, NH_4^+, because the pH is below the pKa of the NH_4^+/NH_3 system (approximately 9.25 at 25 °C in freshwater). Consequently, the proportion of un-ionized NH_3 is expected to be low, and ammonia-related risk should be interpreted in relation to pH and temperature. This input was rapidly mineralized into NH_4^+, which increased during the early culture phase (Figure 3a), peaking between days 10 and 17 (up to 12.38 mg-N/L in Nt_3), before declining toward the end of the experiment (1.56–7.05 mg-N/L at day 42). NH_4^+ production rates followed a similar pattern, with the highest values in nucleotide treatments (0.793–0.917 mg-N/L/day), indicating greater nitrogen excretion associated with higher metabolic activity.

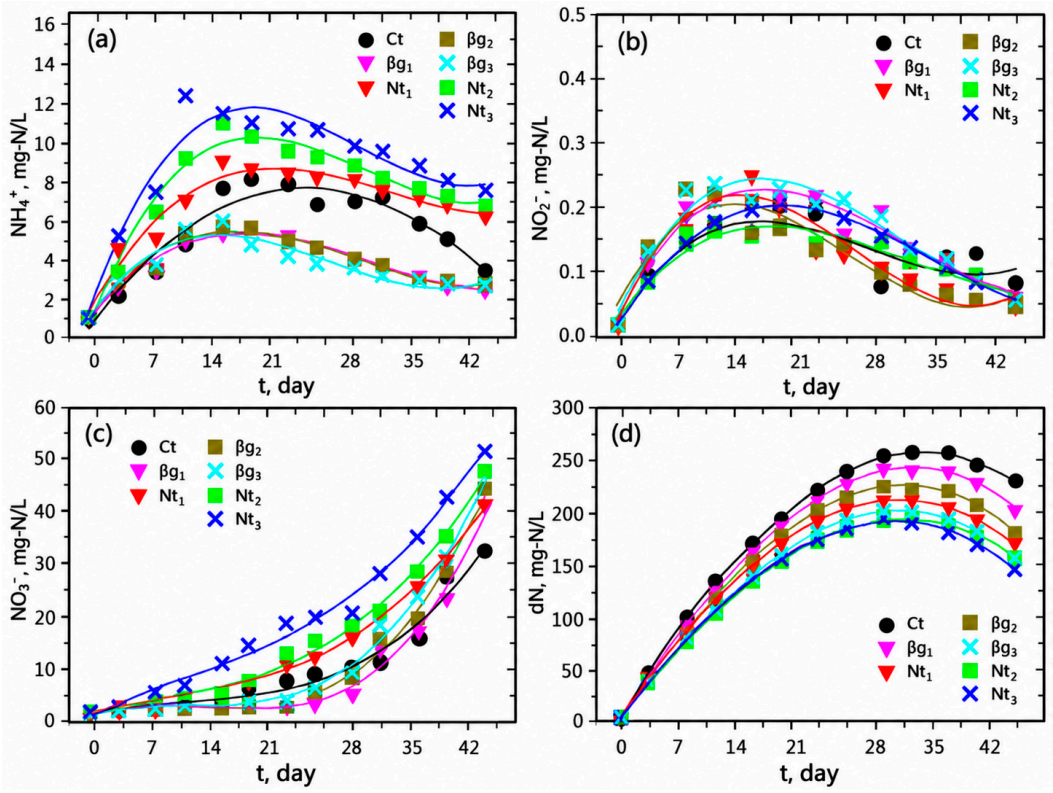


Figure 3. Temporal variations in β-glucan and nucleotide supplementation for (**a**) NH_4^+, (**b**) NO_2, (**c**) NO_3 and (**d**) residual nitrogen fraction during the 42-day Nile Tilapia culture period.

The produced ammonia subsequently served as a substrate for nitrification, leading to transient increases in NO_2^- during the early culture stages (Figure 3b). NO_2^- peaked between days 7 and 17 up to 0.240 mg-N/L in Nt_1, followed by a gradual decline to low levels by day 42 in the range 0.03–0.07 mg-N/L, consistent with apparent conversion of nitrite to nitrate as the experiment progressed. Correspondingly, NO_3^- accumulated continuously throughout the culture period (Figure 3c), reaching final concentrations of 31.74–51.47 mg-N/L, with higher values generally observed in supplemented treatments. These concentration patterns suggest differences in apparent nitrogen transformation dynamics among treatments but do not directly demonstrate nitrifying community activity or establish nitrification as the sole process responsible for these changes [49].

In parallel, the calculated residual nitrogen fraction (dN) showed a distinct temporal pattern, increasing during the early- to mid-culture period and peaking at 229.76 mg-N/L in Ct around day 28 (Figure 3d). This pattern highlights the residual nitrogen pool's contribution to overall nitrogen distribution under ZWE conditions. Differences in dN among treatments reflect variation in nitrogen partitioning, complementing the observed changes in inorganic nitrogen concentrations. Together, these temporal patterns provide insight into treatment-associated nitrogen dynamics and support further interpretation of nitrogen transformation pathways under ZWE conditions. The temporal patterns of nitrogen species were further characterized using cubic regression, as presented in Supplementary File S3.

On day 21, the calculated nitrogen distribution was dominated by the residual nitrogen fraction the nitrogen distribution was dominated by residual nitrogen (dN: 71.63–86.59%), followed by nitrate (NO_3^-: 12.46–26.32%), while ammonia (NH_4^+: 0.90–3.80%) and nitrite (NO_2^-: 0–0.06%) remained minor fractions (Figure 4a–f). The dN proportion indicates the calculated residual pool's relative contribution to the overall nitrogen distribution, whereas the nitrate fraction reflects nitrate's relative contribution to the measured nitrogen profile. In nucleotide treatments, higher supplementation levels were associated with higher nitrate proportions, consistent with the observed nitrate concentration patterns [50].

3.4. Immune System

NBT activity increased in all treatments after 35 days of culture compared with initial values (Figure 5a), indicating an enhanced respiratory burst in immune cells. The Ct showed a moderate increase in the ΔNBT = 0.189, whereas β-glucan treatments exhibited substantially higher responses, particularly in βg_1 at ΔNBT = 0.513, followed by βg_2 and βg_3. Nucleotide supplementation also elevated NBT activity, with the largest increase observed in Nt_1 in the ΔNBT of 0.411, although the magnitude remained lower than that observed in β-glucan treatments. Both dietary additives stimulated innate immune activity, with β-glucan producing a more pronounced enhancement of phagocytic function [51].

SOD activity similarly increased across all treatments (Figure 5c), improving antioxidant defense capacity. The Ct showed the lowest increase (ΔSOD = 0.086), while β-glucan treatments exhibited stronger responses, particularly in βg_1 (ΔSOD = 0.202) and βg_2 (ΔSOD = 0.194). Nucleotide treatments also enhanced SOD activity, with the highest increase observed in Nt_2 (ΔSOD = 0.193), although overall responses were slightly lower than those of β-glucan. Collectively, β-glucan and nucleotide supplementation enhanced resistance to oxidative stress and immune-related activity, with β-glucan consistently inducing a stronger response [52].

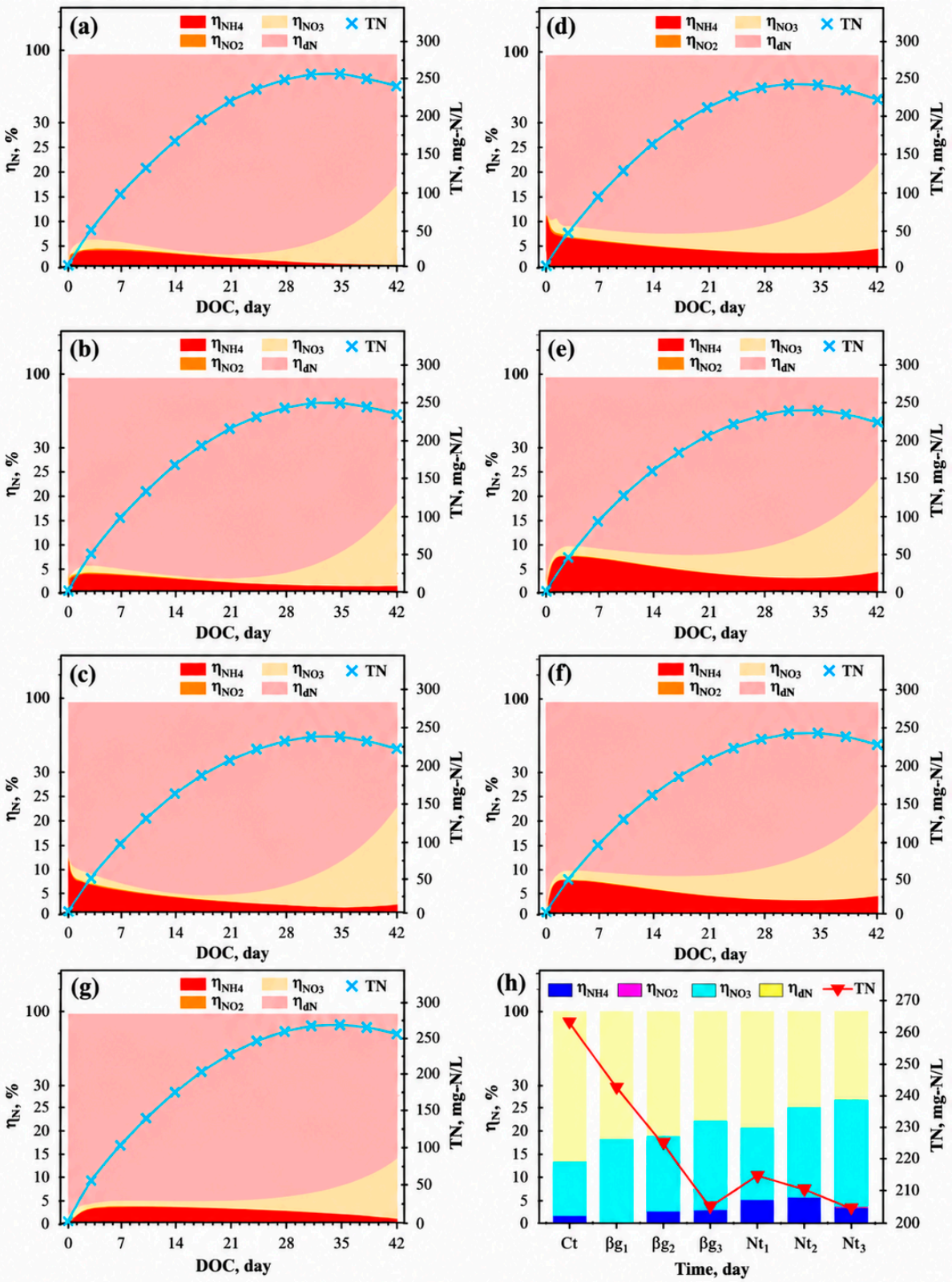


Figure 4. Comparison of nitrogen selectivity effects of functional feed additives: β-glucan at concentrations (**a**) βg_1 = 1%, (**b**) βg_2 = 2%, (**c**) βg_3 = 3%, and nucleotide at concentrations (**d**) Nt_1 = 1%, (**e**) Nt_2 = 2%, (**f**) Nt_3 = 3%, compared to (**g**) the unsupplemented Ct, during the 42-day Nile tilapia culture period under zero-water-exchange conditions; (**h**) comparative nitrogen selectivity across all treatments at day 28.

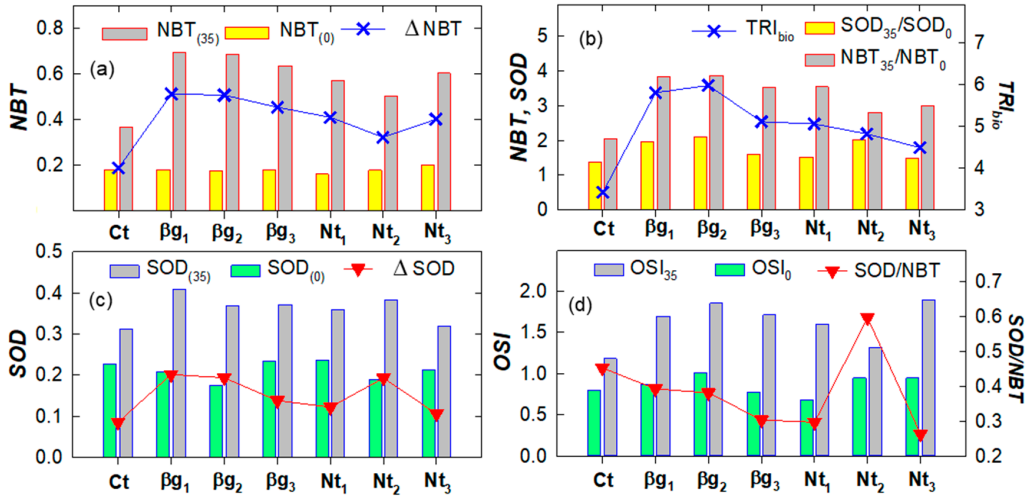


Figure 5. Nitroblue tetrazolium (NBT) and superoxide dismutase (SOD) activities of Nile tilapia at day 0 and day 35 under β-glucan and nucleotide supplementation: (**a**) ΔNBT, (**b**) TRI_{bio}, (**c**) ΔSOD, (**d**) OSI, and AAR.

4. Discussion

4.1. Nitrogen Kinetic Reactions

The nitrogen transformation model was developed based on a sequence of biochemical and microbial processes, beginning with organic nitrogen mineralization and progressing through nitrification and apparent nitrogen transfer (Equations (16)–(20)). These fundamental reactions were simplified into a conceptual reaction scheme for the conversion of organic nitrogen into NH_3/NH_4^+ and its partitioning between nitrification and nitrogen transfer to the residual nitrogen pool processes (Equations (21)–(24)). Within this framework, nitrogen transformation is represented as dynamic partitioning among ammonia, nitrite, nitrate, and residual nitrogen pools. The kinetic model was expressed using a system of differential equations (Equations (25)–(28)), with k_e representing ammonia input or generation, k_1 representing apparent NH_3/NH_4^+ to NO_2^- conversion, k_2 representing apparent NO_2^- to NO_3^- conversion, and k_a representing apparent nitrogen transfer to the residual nitrogen pool. These parameters were derived from the experimental concentration data using the integral-based formulations (Equations (29)–(32)), providing quantitative estimates of the apparent nitrogen transformation dynamics under ZWE conditions.

The process-based kinetic approach was selected to quantitatively describe the temporal partitioning of nitrogen among the measured nitrogen pools under ZWE conditions. The model links the major observed nitrogen pools through sequential transformation pathways, allowing treatment-level quantification of ammonia generation, apparent NH_4^+ to NO_2^- conversion, apparent nitrite-to-nitrate conversion, and transfer of ammonia-derived nitrogen toward the residual nitrogen pool. This formulation was therefore used to compare nitrogen transformation and partitioning dynamics among the β-glucan, nucleotide, and Ct treatments. The kinetic formulation assumed ZWE, constant apparent kinetic coefficients within the analysis interval, and internal nitrogen transformation and partitioning as the principal processes governing changes in the measured nitrogen pools. The residual nitrogen fraction (dN) was treated as an operational mass-balance pool representing nitrogen not accounted for by the measured dissolved inorganic nitrogen species. Accordingly, k_e, k_1, k_2, and k_a were interpreted as model-derived apparent kinetic coefficients representing system-level nitrogen transformation and partitioning.

Nitrogen transformation reactions

$$R - NH_2 + H_2O \rightarrow NH_3 + R - OH \text{ (Protein metabolism)} \quad (16)$$

$$NH_3 + H_2O \leftrightarrow NH_4^+ + OH^- \text{ (In the water)} \quad (17)$$

$$NH_4^+ + 1.5O_2 \rightarrow NO_2^- + H^+ + H_2O \text{ (}Nitrosomonas\text{)} \quad (18)$$

$$NO_2^- + 0.5O_2 \rightarrow NO_3^- \text{ (}Nitrobacter\text{)} \quad (19)$$

$$NH_4^+ + C_{org} + O_2 \rightarrow \text{Biomass} + CO_2 + H_2O \text{ (Apparent nitrogen transfer)} \quad (20)$$

Conceptual nitrogen reaction scheme

$$\text{Organic N} \xrightarrow{k_e} NH_4^+ \quad (21)$$

$$NH_4^+ \xrightarrow{k_1} NO_2^- \quad (22)$$

$$NO_2^- \xrightarrow{k_2} NO_3^- \quad (23)$$

$$NH_4^+ \xrightarrow{k_a} \text{Assimilation (dN)} \quad (24)$$

Nitrogen kinetic model

$$\frac{dNH_4^+}{dt} = k_e - (k_1 + k_a)NH_4^+ \quad (25)$$

$$\frac{dNO_2^-}{dt} = k_1 NH_4^+ - k_2 NO_2^- \quad (26)$$

$$\frac{dNO_3^-}{dt} = k_2 NO_2^- \quad (27)$$

$$\frac{d(dN)}{dt} = k_a NH_4^+ \quad (28)$$

$$k_a = \frac{dN_{(t)} - dN_{(0)}}{\int_0^t NH_{4\,(t)}^+ dt} \quad (29)$$

$$k_2 = \frac{NO_{3(t)}^- - NO_{3(0)}^-}{\int_0^t NO_{2(t)}^- dt} \quad (30)$$

$$k_1 = \frac{NO_{2(t)}^- - NO_{2(0)}^- + k_2 \int_0^t NO_{2(t)}^- dt}{\int_0^t NH_{4(t)}^+ dt} \quad (31)$$

$$k_e = \frac{NH_{4(t)}^+ - NH_{4(0)}^+ + (k_1 + k_a) \int_0^t NH_{4(t)}^+ dt}{\Delta t} \quad (32)$$

The kinetic coefficients were estimated from the temporal nitrogen concentration data using the integral-based formulations presented in Equations (29)–(32). The model-derived kinetic coefficients quantified treatment-associated differences in apparent nitrogen transformation and distribution patterns, complementing observed temporal changes in nitrogen concentrations under ZWE conditions. Parameter estimation was conducted over days 7–30 using the observed changes in NH_4^+, NO_2^-, NO_3^- and residual nitrogen together with the corresponding time-integrated concentrations. The kinetic modeling results revealed distinct differences in the model-derived apparent nitrogen transformation coefficients among treatments (Table 1).

Overall, the model-derived k_1 remained relatively low and within a narrow range (0.062–0.171/day), indicating a comparatively slower conversion of ammonia to nitrite. In contrast, the model-derived k_2 was substantially higher, particularly in nucleotide treatments (Nt_1–Nt_3: 4.994–5.748/day), compared with the control and β-glucan treatments (2.643–4.396/day). This pattern matched the lower terminal NO_2^- concentrations and greater NO_3^- accumulation observed in nucleotide treatments, suggesting greater apparent NO_2^--to-NO_3^- conversion. These concentration patterns, together with the model-derived

apparent kinetic coefficients, characterize differences in nitrogen transformation dynamics but do not directly establish the underlying microbial mechanisms [53].

Table 1. Model-derived apparent kinetic coefficients describing nitrogen transformation in Nile tilapia fed β-glucan- and nucleotide-supplemented diets under zero-water-exchange conditions.

Equations	Ct	βg_1	βg_2	βg_3	Nt_1	Nt_2	Nt_3
$\int_7^{30} NH_{4(t)}^+ dt$	145.794	88.091	101.394	93.407	183.58	221.167	234.795
$\int_7^{30} NO_{2(t)} dt$	3.455	3.966	3.16	4.374	3.44	3.576	4.177
$dN_{(30)} - dN_{(7)}$	160.26	148.85	135.92	120.20	125.38	120.13	111.99
$NO_{3(30)} - NO_{3(7)}$	9.132	11.686	13.892	16.082	17.185	17.513	24.011
$NO_{2(30)} - NO_{2(7)}$	−0.027	−0.066	−0.156	−0.095	−0.097	−0.049	−0.007
$NH_{4(30)}^+ - NH_{4(7)}^+$	4.119	−0.050	0.183	−0.692	2.669	1.867	2.318
k_e, mg/L/day	7.543	6.975	6.514	5.891	6.310	6.064	6.014
k_1/day	0.062	0.132	0.135	0.171	0.093	0.079	0.102
k_2/day	2.643	2.948	4.396	3.676	4.994	4.897	5.748
k_a/day	1.099	1.690	1.341	1.287	0.683	0.543	0.477

The model-derived apparent kinetic coefficients provide a quantitative comparison of nitrogen transformation patterns among dietary treatments. Considered alongside the observed nitrogen concentration profiles and model-fit indicators (R^2 and RMSE), these coefficients characterize treatment-associated differences in nitrogen dynamics under zero-water-exchange conditions. The model yielded R^2 values of 0.786–0.999 and RMSE values of 0.003–9.578 mg/L across treatments and nitrogen pools, indicating generally close agreement between observed and model-predicted temporal nitrogen dynamics (Supplementary File S4).

In parallel, the model-derived k_a and k_e revealed distinct nitrogen partitioning patterns among treatments. β-glucan treatments exhibited higher k_a values (1.287–1.690/day) than nucleotide treatments (0.477–0.683/day), indicating greater apparent transfer of ammonia-derived nitrogen toward the residual nitrogen pool. Conversely, nucleotide treatments showed higher k_e values (6.014–6.310/day) and higher k_2 values (4.994–5.748/day), indicating greater apparent nitrogen input to the ammonia pool and subsequent NO_2^- to NO_3^- turnover, respectively. These contrasting kinetic patterns indicate that β-glucan supplementation favored apparent nitrogen transfer toward the residual pool, whereas nucleotide supplementation favored apparent oxidized-nitrogen turnover, consistent with the greater nitrate accumulation observed in nucleotide treatments [23,54].

The contrasting k_a and k_e values further illustrate differences in apparent nitrogen partitioning among treatments. β-glucan treatments exhibited higher k_a values (1.287–1.690/day) than nucleotide treatments (0.477–0.683/day), indicating greater apparent transfer of ammonia-derived nitrogen to the modeled residual nitrogen pool. Because k_a was inferred from temporal concentration changes, this pattern represents an apparent system-level partitioning of nitrogen rather than direct evidence of microbial nitrogen use, microbial biomass formation, or nitrogen incorporation into fish tissue. Conversely, nucleotide treatments showed relatively high k_e values (6.014–6.310/day) and higher k_2 values (4.994–5.748/day), indicating greater apparent nitrogen input to the ammonia pool and greater apparent NO_2^- to NO_3^- turnover. Kinetic patterns suggest that β-glucan favored apparent nitrogen transfer toward the residual nitrogen pool, whereas nucleotide favored apparent oxidized-nitrogen turnover, consistent with the greater NO_3^- accumulation [11,54].

4.2. Coupling of Nitrogen Kinetics, Oxidative Stress, and Immune Response

The increase in OSI (Figure 5b) and consistently high TRI values (Figure 5d) coincided with variations in NBT and SOD responses across treatments, suggesting an association between nitrogen-related indices and physiological responses in the ZWE system. The model-derived apparent kinetic coefficients (*ke*, k_1, and k_2) differed among treatments and were accompanied by changes in nitrogen species and physiological indicators. The ΔOSI/ΔNBT ratio further characterized the relative antioxidant and respiratory burst responses among treatments (Figure 6). β-glucan treatments showed ratios of 0.304–0.393 alongside higher model-derived apparent nitrogen transfer coefficients (k_a), whereas nucleotide treatments exhibited distinct response patterns, particularly Nt_3 (0.263; $OSI = 1.89$). The Nt_2 with OSI = 0.597 demonstrated the most efficient antioxidant adaptation among treatments. Oxidative status in Nile tilapia is driven by the interplay between nitrogen kinetics and physiological regulation, with the balance between ROS generation and antioxidant capacity determining the fish's resilience under intensive ZWE conditions [54].

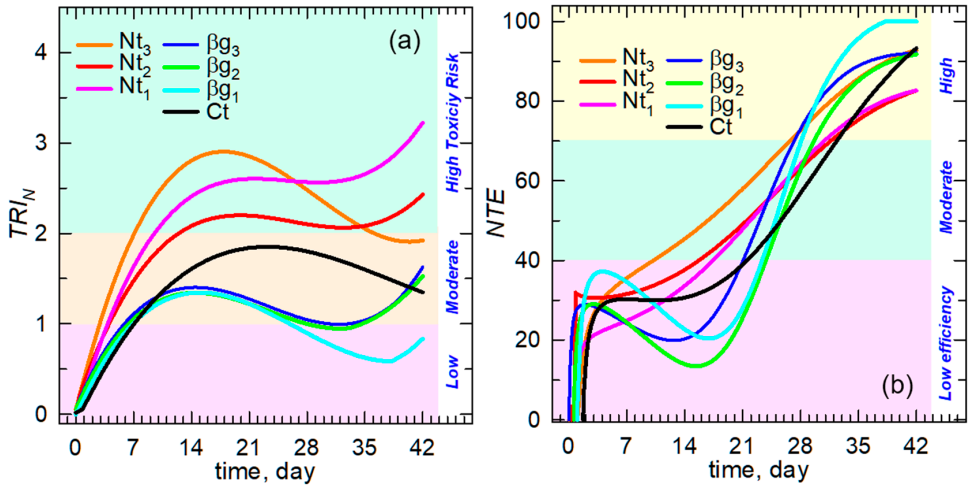


Figure 6. Temporal dynamics of (**a**) nitrogen Toxicity Risk Index (TRI_N) over time, and (**b**) presents Nitrogen Transformation Efficiency (NTE, %) as a function of time on β-glucan and nucleotide feed additive.

4.3. Integrated Toxicity Risk, Nitrogen Transformation Efficiency, and Physiological Response

The temporal profiles of the TRI_N revealed a pronounced initial toxicity peak across all treatments, followed by a gradual decline toward the end of the culture period (Figure 6a). At early stages (days 1–5), TRI_N values were consistently high (>2), indicating acute toxicity risk driven by elevated NH_4^+ and NO_3^-, which are well-known to disrupt ion regulation and oxygen transport in fish. This phase coincides with the accumulation of reduced nitrogen forms before efficient nitrification is established [55]. Subsequently, TRI_N declined steadily across treatments, reaching moderate levels (1–2) by day 42, reflecting the progressive conversion of toxic intermediates into NO_3^-. This trend is strongly supported by the NTE, which increased over time from moderate or even negative values in early stages to high efficiency (>90%) at the end of the experiment (Figure 6b). Notably, nucleotide treatments (Nt_2 and Nt_3) exhibited faster increases in NTE, reaching >95% by day 42, consistent with their higher k_2, which were associated with lower NO_2^- concentration and reduced toxicity. In contrast, β-glucan treatments showed a more gradual improvement, reflecting a more balanced partitioning between nitrification (k_1 and k_2) and nitrogen transfer (k_a), which contributed to system stability rather than rapid oxidation [56]. Nitrogen accumulation is an inherent environmental challenge in ZWE systems that may increase physiological

stress, while β-glucan and nucleotide supplementation may help fish cope by supporting immune function and antioxidant defense, as reflected in NBT and SOD activities.

These nitrogen dynamics were closely linked to physiological responses, particularly oxidative stress and immune activation. The early high TRI_N phase likely triggered elevated ROS production, as reflected by increased NBT activity, while the concurrent rise in SOD indicates an adaptive antioxidant response to mitigate oxidative damage [57]. Treatments with faster toxicity decline (Nt_2 and Nt_3) likely reduced prolonged exposure to oxidative stress, but may have experienced sharper initial stress due to delayed NH_4^+ oxidation (lower k_1) and rapid NO_2^- turnover (high k_2). Conversely, β-glucan treatments, characterized by lower nitrogen release (k_e) and more moderated kinetics, likely provided a more stable physiological environment, supporting sustained immune activation with lower fluctuation in stress intensity [58]. From an operational perspective, water management strategies should target the early culture phase (approximately days 1–10), when TRI_N peaks and toxicity risk are highest. Partial water exchange during this critical window could dilute toxic nitrogen species, while enhanced aeration could support nitrification by improving oxygen availability, thereby helping to reduce acute stress and improve overall system resilience [59].

4.4. Integrated Effects of Nucleotide Supplementation on Nitrogen Dynamics, Water Quality, and Fish Physiology

Nucleotide supplementation improved growth performance and altered nitrogen dynamics in the ZWE system (Table 2). The complete ANOVA results, including the original data, are provided in Supplementary File S5. These responses may reflect the physiological roles of dietary nucleotides in supporting nucleic acid synthesis, cellular metabolism, and tissue growth, as reported in previous studies [44]. In addition, intestinal function is closely related to nutrient digestion and absorption, and dietary nucleotide supplementation has been suggested to support intestinal integrity and digestive function in fish. These physiological processes plausibly explain the improved production performance observed in the supplemented groups. The observed responses suggest that β-glucan and nucleotide supplementation may support immune activity and antioxidant defense despite fluctuations in nitrogen concentrations. These findings highlight the potential benefits of functional feed supplementation in ZWE aquaculture, while emphasizing that effective nitrogen and water-quality management remains essential to maintain favorable rearing conditions.

From a kinetic perspective, this behavior was characterized by higher model-derived k_e coefficients in nucleotide treatments, along with higher conversion coefficients. The higher k_2 values indicate higher apparent turnover of nitrite to nitrate. In contrast, β-glucan treatments exhibited higher model-derived apparent nitrogen transfer coefficients (k_a), indicating greater apparent transfer of ammonia-derived nitrogen toward the residual nitrogen pool. These contrasting kinetic patterns were accompanied by changes in DO and pH over the culture period, reflecting the interaction between nitrogen transformation and water quality under ZWE conditions [20].

At the organism level, these environmental and kinetic interactions were reflected in growth and immune responses. Nucleotide supplementation improved growth performance by boosting metabolic activity, while the observed nitrogen concentration patterns and model-derived apparent kinetic coefficients were consistent with differences in nitrogen transformation dynamics among treatments. At the same time, higher SOD and NBT levels indicate a coordinated physiological response, in which increased ROS production is balanced by enhanced antioxidant and immune functions. Overall, nucleotide supplementation was associated with distinct nitrogen transformation patterns and improved growth performance, whereas β-glucan was associated with greater apparent transfer of

ammonia-derived nitrogen toward the modeled residual nitrogen pool. These findings highlight the potential of functional feed supplementation to influence nitrogen dynamics, water quality, and fish performance in intensive ZWE aquaculture systems.

Table 2. Water quality, nitrogen dynamics, growth performance, and immune responses of Nile tilapia under ZWE conditions with β-glucan (βg_1–βg_3) and nucleotide (Nt_1–Nt_3) supplementation compared to the control (Ct).

Parameter	Ct	Bg_1	Bg_2	Bg_3	Nt_1	Nt_2	Nt_3
T, °C	26.12 ± 0.06 ^{a}	26.03 ± 0.18 ^{a}	25.96 ± 0.36 ^{a}	25.87 ± 0.24 ^{a}	25.77 ± 0.42 ^{a}	25.84 ± 0.33 ^{a}	25.61 ± 0.38 ^{a}
DO, mg/L	6.40 ± 0.09 ^{a}	6.54 ± 0.08 ^{a}	6.26 ± 0.32 ^{a}	6.34 ± 0.39 ^{a}	6.24 ± 0.33 ^{a}	6.04 ± 0.32 ^{a}	6.14 ± 0.34 ^{a}
pH	6.48 ± 0.19 ^{a}	6.77 ± 0.29 ^{a}	6.42 ± 0.14 ^{a}	6.67 ± 0.26 ^{a}	6.76 ± 0.08 ^{a}	6.76 ± 0.21 ^{a}	6.79 ± 0.04 ^{a}
NH_4^+, mg N/L	4.34 ± 0.68 ^{ab}	2.28 ± 0.57 ^{a}	3.50 ± 0.16 ^{ab}	2.71 ± 1.16 ^{a}	5.18 ± 1.69 ^{bc}	7.18 ± 0.91 ^{cd}	8.39 ± 0.09 ^{d}
NO_2^-, mg N/L	0.10 ± 0.04 ^{a}	0.15 ± 0.02 ^{a}	0.13 ± 0.02 ^{a}	0.14 ± 0.02 ^{a}	0.13 ± 0.07 ^{a}	0.11 ± 0.01 ^{a}	0.12 ± 0.02 ^{a}
NO_3^-, mg N/L	9.86 ± 0.89 ^{a}	9.03 ± 1.26 ^{a}	10.84 ± 0.42 ^{ab}	12.08 ± 0.89 ^{b}	15.28 ± 0.19 ^{c}	16.73 ± 1.15 ^{c}	22.05 ± 0.92 ^{d}
dN, mg N/L	181.08 ± 0.53 ^{f}	169.68 ± 1.97 ^{e}	155.84 ± 3.14 ^{d}	142.58 ± 5.58 ^{bc}	149.04 ± 4.82 ^{cd}	139.30 ± 3.55 ^{ab}	131.59 ± 2.72 ^{a}
W, g	14.18 ± 0.06 ^{a}	15.46 ± 0.36 ^{b}	15.69 ± 0.80 ^{b}	16.43 ± 0.37 ^{b}	16.35 ± 0.30 ^{b}	17.49 ± 0.36 ^{c}	18.60 ± 0.48 ^{d}
L, cm	8.94 ± 0.36 ^{a}	9.19 ± 0.45 ^{a}	9.07 ± 0.38 ^{a}	9.26 ± 0.42 ^{a}	9.42 ± 0.30 ^{a}	9.83 ± 0.09 ^{a}	9.63 ± 0.35 ^{a}
SR, %	96.19 ± 0.03 ^{c}	97.74 ± 0.00 ^{c}	96.49 ± 0.04 ^{c}	92.02 ± 0.03 ^{a}	95.53 ± 0.03 ^{b}	92.21 ± 0.05 ^{a}	91.08 ± 0.05 ^{a}
NBT, OD unit	0.36 ± 0.02 ^{a}	0.74 ± 0.04 ^{d}	0.67 ± 0.07 ^{cd}	0.67 ± 0.02 ^{cd}	0.59 ± 0.02 ^{bc}	0.53 ± 0.10 ^{b}	0.58 ± 0.01 $^{b\,c}$
SOD, U/mL	0.28 ± 0.05 ^{a}	0.43 ± 0.03 ^{a}	0.34 ± 0.20 ^{a}	0.51 ± 0.11 ^{a}	0.24 ± 0.10 ^{a}	0.49 ± 0.12 ^{a}	0.37 ± 0.03 ^{a}

Values are mean ± SD based on three replicate tanks per treatment ($n = 3$). Different superscript letters within rows indicate significant differences ($p < 0.05$).

5. Conclusions

This study demonstrated that β-glucan and nucleotide supplementation distinctly modified nitrogen transformation and physiological responses in Nile tilapia under ZWE conditions. Nucleotide supplementation, particularly Nt_3, enhanced fish growth, with final weight reaching 28.32 g, while cumulative feed-derived nitrogen was lower than in the control. Nucleotide treatments also exhibited higher model-derived apparent NO_2^- to NO_3^- conversion coefficients (k_2 = 4.994–5.748/day), accompanied by greater nitrate accumulation and lower terminal nitrite concentrations. In contrast, β-glucan treatments showed higher model-derived apparent nitrogen transfer coefficients (k_a = 1.287–1.690/day), consistent with greater transfer of ammonia-derived nitrogen toward the residual nitrogen pool. Overall, nucleotide supplementation favored apparent oxidized-nitrogen turnover, whereas β-glucan was associated with greater apparent nitrogen transfer toward the residual nitrogen pool and stronger physiological regulation.

Supplementary Materials: The following supporting information can be downloaded at https://www.mdpi.com/article/10.3390/nitrogen7040129/s1: Supplementary File S1 (Water Quality Monitoring), Supplementary File S2 (Nitrogen Observation), Supplementary File S3 (Nitrogen Fitting Equations), Supplementary File S4 (Model parameter optimization), Supplementary File S5 (Statistical Analysis).

Author Contributions: The authors confirm their contributions to the paper as follows: Collection and assembly of data, data analysis and interpretation, writing the article: R.Y.; Research concept and design, writing the article, Critical revision of the article, and Final approval of the article: S.S.P.R.; Analysis and interpretation of results: I.M.D.M., H.S., A.P., A.R. and A.M.H. All authors have read and agreed to the published version of the manuscript.

Funding: This research was funded by Universitas Brawijaya through the Penelitian Dasar Madya (PDM) scheme, Fiscal Year 2025, under Research Contract No. 00738.61/UN10.A0501/B/PT.01.03.2/2025.

Data Availability Statement: The authors declare that all data discussed in the study are available in the manuscript.

Acknowledgments: We sincerely appreciate Brawijaya University for invaluable support through the research grant. We also thank all individuals and organizations whose contributions enriched this research endeavor.

Conflicts of Interest: The authors declare no conflicts of interest.

References

1. Ahmad, I.; Rani, A.; Verma, A.; Maqsood, M. Biofloc technology: An emerging avenue in aquatic animal healthcare and nutrition. *Aquac. Int.* **2017**, *25*, 1215–1226. [CrossRef]
2. Edwards, T.M.; Puglis, H.J.; Kent, D.B.; Jonathan, L.; Bradshaw, L.M.; Farag, A.M. Ammonia and aquatic ecosystems—A review of global sources, biogeochemical cycling, and effects on fish. *Sci. Total Environ.* **2024**, *907*, 167911. [CrossRef] [PubMed]
3. Huang, Y.; Liu, M.; Jiang, K.; Zhong, C.; Xu, K.; Wang, B.; Wang, L. The dynamic features and microbial mechanism of nitrogen transformation in small greenhouse farming system of Pacific white shrimp, *Litopenaeus vannamei*. *Aquaculture* **2025**, *605*, 742557. [CrossRef]
4. Sriprateep, K.; Pitakaso, R.; Khonjun, S.; Luesak, P.; Jutagate, A.; Kaewta, C.; Srichok, T.; Kosacka-Olejnik, M.; Matitopanum, S. Optimizing Nile Tilapia growth and production costs in earthen ponds using multi-objective adaptive artificial intelligence systems. *Aquac. Rep.* **2025**, *41*, 102716. [CrossRef]
5. Zhang, A.; Shen, H.; Zhang, X.; Wang, T.; Mei, F.; Jeyakumar, D.T.; Fang, F.; Qin, W.; Xu, Z. The role of microalgae in *Penaeus vannamei* aquaculture: Exploring the importance of biofloc technology. *Aquaculture* **2025**, *603*, 742397. [CrossRef]
6. Robles-Porchas, G.; Gollas-Galván, T.; Martínez-Porchas, M.; Martínez-Córdova, L.; Miranda-Baeza, A.; Vargas-Albores, F. The nitrification process for nitrogen removal in biofloc system aquaculture. *Rev. Aquac.* **2020**, *12*, 2228–2249. [CrossRef]
7. Xu, W.; Xu, Y.; Su, H.; Hu, X.; Yang, K.; Wen, G.; Cao, Y. Characteristics of Ammonia Removal and Nitrifying Microbial Communities in a Hybrid Biofloc-RAS for Intensive *Litopenaeus vannamei* Culture: A Pilot-Scale Study. *Water* **2020**, *12*, 3000. [CrossRef]
8. Mao, J.; Ren, M.; Gong, J.; Qian, Y. The influence of temperature and nitrogen source on ammonia removal and associated metabolism in activated sludge process for high-salinity nitrogen-containing wastewater treatment. *J. Water Process Eng.* **2026**, *81*, 109269. [CrossRef]
9. Li, W.; Jiang, X.; Li, J.; Li, J. Simultaneous aerobic nitrogen and phosphorous removal characteristics and mechanism by heterotrophic nitrification aerobic denitrification microorganisms: A review. *J. Water Process Eng.* **2025**, *76*, 108235. [CrossRef]
10. Li, W.; Shang, S.; Yu, J.; Zhang, K.; Cui, Y.; Zhou, S. Research progress of direct ammonia oxidation (Dirammox) in biological nitrogen removal: Insight from genetic basis, biochemical mechanism and potential applications. *J. Water Process Eng.* **2026**, *87*, 110038. [CrossRef]
11. Rahardjo, S.S.P.; Shih, Y.-J.; Wu, Z.-L. Modulating tenorite-based bimetallic electrocatalysts for highly selective ammonia oxidation to N2. *J. Hazard. Mater.* **2026**, *512*, 142323. [CrossRef] [PubMed]
12. Gymnastiar, A.A.; Yuniarti, A.; Rahardjo, S.S.P.; Maimunah, Y.; Yuwanita, R.; Mahariawan, I.M.D.; Widyawati, Y.; Sholichin, M.; Hariati, A.M. The role of Pure Nano Oxygen Bubbles in the nitrogen cycle of tilapia biofloc systems. *Chemosphere* **2025**, *384*, 144522. [CrossRef] [PubMed]
13. Preena, P.; Kumar, V.; Singh, I. Nitrification and denitrification in recirculating aquaculture systems: The processes and players. *Rev. Aquac.* **2021**, *13*, 2053–2075. [CrossRef]
14. Rohani, M.; Islam, S.; Hossain, M.; Ferdous, Z.; Siddik, M.; Nuruzzaman, M.; Padeniya, U.; Brown, C.; Shahjahan, M. Probiotics, prebiotics and synbiotics improved the functionality of aquafeed: Upgrading growth, reproduction, immunity and disease resistance in fish. *Fish Shellfish Immunol.* **2021**, *120*, 569–589. [CrossRef] [PubMed]
15. Dalmo, R.; Bøgwald, J. Beta-glucans as conductors of immune symphonies. *Fish Shellfish Immunol.* **2008**, *25*, 384–396. [CrossRef] [PubMed]
16. Deng, M.; Dai, Z.; Song, K.; Wang, Y.; He, X. Integrating Microbial Protein Production and Harvest Systems into Pilot-Scale Recirculating Aquaculture Systems for Sustainable Resource Recovery: Linking Nitrogen Recovery to Microbial Communities. *Environ. Sci. Technol.* **2021**, *55*, 16735–16746. [CrossRef] [PubMed]
17. Liu, H.; Li, J.; Guo, X.; Liang, Y.; Wang, W. Yeast culture dietary supplementation modulates gut microbiota, growth, and biochemical parameters of grass carp. *Microb. Biotechnol.* **2018**, *11*, 551–565. [CrossRef] [PubMed]
18. Matassa, S.; Verstraete, W.; Pikaar, I.; Boon, N. Autotrophic nitrogen assimilation and carbon capture for microbial protein production by a novel enrichment of hydrogen-oxidizing bacteria. *Water Res.* **2016**, *101*, 137–146. [CrossRef] [PubMed]

19. Zeng, L.; Wang, Y.; Ai, C.; Zhang, J. Differential effects of β-glucan on oxidative stress, inflammation and copper transport in two intestinal regions of large yellow croaker *Larimichthys crocea* under acute copper stress. *Ecotoxicol. Environ. Saf.* **2018**, *165*, 78–87. [CrossRef] [PubMed]
20. Liu, L.; Fang, J.; Liang, X.; He, S. Nucleotide promotes feed intake and protein utilization via regulating the gene expression of feeding and nitrogen metabolism in juvenile Chinese perch (*Siniperca chuatsi*). *Aquac. Nutr.* **2020**, *26*, 1702–1712. [CrossRef]
21. Nootong, K.; Pavasant, P.; Powtongsook, S. Effects of Organic Carbon Addition in Controlling Inorganic Nitrogen Concentrations in a Biofloc System. *J. World Aquac. Soc.* **2011**, *42*, 339–346. [CrossRef]
22. Xiao, W.; Sun, R.; Ran, L.; Zhang, Z.; Bai, X.; Lv, C.; Zhang, M.; Hu, S.; Wu, Y. Response of nitrogen transformation and microbial community to aromatic compounds stress along heterotrophic nitrification and aerobic denitrification process. *Environ. Res.* **2025**, *285*, 122413. [CrossRef] [PubMed]
23. Rahardjo, S.S.P.; Shih, Y.-J.; Fan, C.-S. Ammonia oxidation by in-situ chloride electrolysis in etching wastewater of semiconductor manufacturing using RuSnOx/Ti electrode: Effect of plating mode and metal ratio. *J. Hazard. Mater.* **2024**, *469*, 134042. [CrossRef] [PubMed]
24. Rahardjo, S.S.P.; Shih, Y.-J. Electrochemical characteristics of silver/nickel oxide (Ag/Ni) for direct ammonia oxidation and nitrogen selectivity in paired electrode system. *Chem. Eng. J.* **2023**, *452*, 139370. [CrossRef]
25. Fajaria, F.N.; Rahardjo, S.S.P.; Fadjar, M.; Supriatin, F.E.; Yuwanita, R.; Pratiwi, A. Oxygen–nutrient constraints on aquaculture carrying capacity in Lahor Reservoir, Indonesia. *Egypt. J. Aquat. Biol. Fish.* **2026**, *30*, 455–470. [CrossRef]
26. Moghaddam, R.; Christianson, L.E. Enhancing nitrate removal in denitrifying woodchip bioreactors: A comprehensive analysis of enhancement strategies and environmental trade-offs. *J. Water Process Eng.* **2025**, *78*, 108806. [CrossRef]
27. Soudagar, M.E.M.; Kiong, T.S.; Jathar, L.; Ghazali, N.N.N.; Ramesh, S.; Awasarmol, U.; Ong, H.C. Perspectives on cultivation and harvesting technologies of microalgae, towards environmental sustainability and life cycle analysis. *Chemosphere* **2024**, *353*, 141540. [CrossRef] [PubMed]
28. Khatun, S.; Rajak, P. In silico study unveils catalase and superoxide dismutase-1 as the potential sub-cellular targets of microplastic-associated compounds and their relevance to oxidative stress. *J. Hazard. Mater. Plast.* **2026**, *3*, 100049. [CrossRef]
29. Vera-Jimenez, N.I.; Pietretti, D.; Wiegertjes, G.F.; Nielsen, M.E. Comparative study of β-glucan induced respiratory burst measured by nitroblue tetrazolium assay and real-time luminol-enhanced chemiluminescence assay in common carp (*Cyprinus carpio* L.). *Fish Shellfish Immunol.* **2013**, *34*, 1216–1222. [CrossRef] [PubMed]
30. Abdellatef, A.A.; Khalil, A.A. Ameliorated effects of *Lactobacillus delbrueckii* subsp. *lactis* DSM 20076 and *Pediococcus acidilactici* NNRL B-5627 on fumonisin B1-induced hepatotoxicity and nephrotoxicity in rats. *Asian J. Pharm. Sci.* **2016**, *11*, 326–336. [CrossRef]
31. American Public Health Association (APHA); American Water Works Association (AWWA); Water Environment Federation (WEF). *Standard Methods for the Examination of Water and Wastewater*, 23rd ed.; American Public Health Association: Washington, DC, USA, 2017; 1796p.
32. U.S. Environmental Protection Agency (USEPA). *Risk Assessment Guidance for Superfund, Volume I: Human Health Evaluation Manual (Part A), Interim Final*; EPA/540/1-89/002; Office of Emergency and Remedial Response: Washington, DC, USA, 1989; 298p.
33. Rowland, M.; Tozer, T.N. *Clinical Pharmacokinetics and Pharmacodynamics: Concepts and Applications*, 4th ed.; Wolters Kluwer Health/Lippincott Williams & Wilkins: Philadelphia, PA, USA, 2011; 839p.
34. Ukeda, H.; Maeda, S.; Ishii, T.; Sawamura, M. Spectrophotometric assay for superoxide dismutase based on tetrazolium salt reduction by xanthine–xanthine oxidase. *Anal. Biochem.* **1997**, *251*, 206–209. [CrossRef] [PubMed]
35. Erel, O. A new automated colorimetric method for measuring total oxidant status. *Clin. Biochem.* **2005**, *38*, 1103–1111. [CrossRef] [PubMed]
36. Evans, J.J.; Pasnik, D.J.; Brill, G.C.; Klesius, P.H. Un-ionized ammonia exposure in Nile tilapia: Toxicity, stress response, and susceptibility to Streptococcus agalactiae. *N. Am. J. Aquac.* **2006**, *68*, 23–33. [CrossRef]
37. Silva, F.J.R.d.; Lima, F.R.d.S.; Vale, D.A.d.; Sá, M.V.d.C.e. High levels of total ammonia nitrogen as NH_4^+ are stressful and harmful to the growth of Nile tilapia juveniles. *Acta Sci. Biol. Sci.* **2013**, *35*, 475–481. [CrossRef]
38. Yildiz, H.Y.; Köksal, G.; Borazan, G.; Benli, Ç.K. Nitrite-induced methemoglobinemia in Nile tilapia, *Oreochromis niloticus*. *J. Appl. Ichthyol.* **2006**, *22*, 427–429. [CrossRef]
39. Monsees, H.; Klatt, L.; Kloas, W.; Wuertz, S. Chronic exposure to nitrate significantly reduces growth and affects the health status of juvenile Nile tilapia (*Oreochromis niloticus* L.) in recirculating aquaculture systems. *Aquac. Res.* **2017**, *48*, 3482–3492. [CrossRef]
40. Escher, B.I.; Hermens, J.L.M. Modes of action in ecotoxicology: Their role in body burdens, species sensitivity, QSARs, and mixture effects. *Environ. Sci. Technol.* **2002**, *36*, 4201–4217. [CrossRef] [PubMed]
41. Nguyen, T.; Koyama, M.; Nakasaki, K. Effects of oxygen supply rate on organic matter decomposition and microbial communities during composting in a controlled lab-scale composting system. *Waste Manag.* **2022**, *153*, 275–282. [CrossRef] [PubMed]
42. Amirkolaie, A.K. Reduction in the environmental impact of waste discharged by fish farms through feed and feeding. *Rev. Aquac.* **2011**, *3*, 19–26. [CrossRef]

43. Li, Q.; Xu, Y.; Liang, C.; Peng, L.; Zhou, Y. Nitrogen removal by algal-bacterial consortium during mainstream wastewater treatment: Transformation mechanisms and potential N2O mitigation. *Water Res*. **2023**, *235*, 119890. [CrossRef] [PubMed]
44. Nguyen, T.; Koyama, M.; Nakasaki, K. Effect of oxygen deficiency on organic matter decomposition during the early stage of composting. *Waste Manag*. **2023**, *160*, 43–50. [CrossRef] [PubMed]
45. Shangguan, H.; Fu, T.; Shen, C.; Mi, H.; Wei, J.; Tang, J.; Zhou, S. In situ generated oxygen distribution causes maturity differentiation during electrolytic oxygen aerobic composting. *Sci. Total Environ*. **2022**, *850*, 157939. [CrossRef] [PubMed]
46. Du, R.; Peng, Y.; Cao, S.; Li, B.; Wang, S.-Y.; Niu, M. Mechanisms and microbial structure of partial denitrification with high nitrite accumulation. *Appl. Microbiol. Biotechnol*. **2015**, *100*, 2011–2021. [CrossRef] [PubMed]
47. Fu, K.; Bian, Y.; Yang, F.; Xu, J.; Qiu, F. Achieving partial nitrification: A strategy for washing NOB out under high DO condition. *J. Environ. Manag*. **2023**, *347*, 119186. [CrossRef] [PubMed]
48. Krishnan, R.; Jang, Y.-S.; Oh, M. Beta glucan induced immune priming protects against nervous necrosis virus infection in sevenband grouper. *Fish Shellfish Immunol*. **2022**, *121*, 163–171. [CrossRef] [PubMed]
49. Abdelmawgood, I.A.; Kotb, M.A.; Ashry, H.; Ebeed, B.W.; Mahana, N.A.; Mohamed, A.S.; Eid, J.; Ramadan, M.A.; Rabie, N.S.; Mohamed, M.Y.; et al. β-glucan mitigates ovalbumin-induced airway inflammation by preventing oxidative stress and CD8+ T cell infiltration. *Int. Immunopharmacol*. **2024**, *132*, 111985. [CrossRef] [PubMed]
50. Wylie, D.A.; Sartaj, M.; Foruzanmehr, R. Ammonia removal from aqueous solution using novel biosorbent developed from TEMPO oxidized flax fibres. *J. Water Process Eng*. **2025**, *71*, 107322. [CrossRef]
51. Bal, Y.; Pak, B.A.; Bayrakdar, A.; Sahinkaya, E. Optimization of moving bed membrane bioreactor process for improved water and nutrient recovery from domestic wastewater. *J. Water Process Eng*. **2025**, *70*, 106934. [CrossRef]
52. Liu, C.; Yao, A.; Li, W.; Xu, Q.; Yang, L.; Ge, Y.; Lan, J.; Lin, S.; Qiu, J. Design of GO@TiO2 and PDA@CNC decorated gelatin aerogel for efficient adsorption and photocatalytic degradation of organic pollutants. *J. Water Process Eng*. **2025**, *75*, 108024. [CrossRef]
53. Silva, M.J.D.S.; Da Costa, F.F.B.; Leme, F.; Takata, R.; Costa, D.C.; Mattioli, C.; Luz, R.K.; Miranda-Filho, K.C. Biological responses of Neotropical freshwater fish *Lophiosilurus alexandri* exposed to ammonia and nitrite. *Sci. Total Environ*. **2018**, *616–617*, 1566–1575. [CrossRef] [PubMed]
54. Orellana-Macías, J.M.; Roselló, M.P.J.; Causapé, J. A Methodology for Assessing Groundwater Pollution Hazard by Nitrates from Agricultural Sources: Application to the Gallocanta Groundwater Basin (Spain). *Sustainability* **2021**, *13*, 6321. [CrossRef]
55. De Felice, B.; Damiano, S.; Montanino, C.; Del Buono, A.; La Rosa, G.; Guida, B.; Santillo, M. Effect of beta- and alpha-glucans on immune modulating factors expression in enterocyte-like Caco-2 and goblet-like LS 174T cells. *Int. J. Biol. Macromol*. **2020**, *153*, 600–607. [CrossRef] [PubMed]
56. Liu, R.; Peng, L.; Zhou, L.; Huang, Z.; Zhou, C.; Huang, C. Oxidative Stress in Cancer Immunotherapy: Molecular Mechanisms and Potential Applications. *Antioxidants* **2022**, *11*, 853. [CrossRef] [PubMed]
57. Zhang, Q.; Chen, H.; Huang, D.-Y.; Xu, C.; Zhu, H.-H.; Zhu, Q. Water managements limit heavy metal accumulation in rice: Dual effects of iron-plaque formation and microbial communities. *Sci. Total Environ*. **2019**, *687*, 790–799. [CrossRef] [PubMed]
58. Seward, E.; Kelly, S. Dietary nitrogen alters codon bias and genome composition in parasitic microorganisms. *Genome Biol*. **2016**, *17*, 226. [CrossRef] [PubMed]
59. Hu, P.; Qian, Y.; Liu, J.; Gao, L.; Li, Y.; Xu, Y.; Wu, J.; Hong, Y.; Ford, T.; Radian, A.; et al. Delineation of the complex microbial nitrogen-transformation network in an anammox-driven full-scale wastewater treatment plant. *Water Res*. **2023**, *235*, 119799. [CrossRef] [PubMed]

Disclaimer/Publisher's Note: The statements, opinions and data contained in all publications are solely those of the individual author(s) and contributor(s) and not of MDPI and/or the editor(s). MDPI and/or the editor(s) disclaim responsibility for any injury to people or property resulting from any ideas, methods, instructions or products referred to in the content.